

Prediction of response spectra via real-time earthquake measurements

Vincenzo Convertito^{a,*}, Iunio Iervolino^b, Aldo Zollo^c, Gaetano Manfredi^b

^a*Istituto Nazionale di Geofisica e Vulcanologia – Osservatorio Vesuviano, RISSC – Lab, Via Coroglio 156, 80124 Napoli, Italy*

^b*Dipartimento di Ingegneria Strutturale, Università di Napoli Federico II, Via Claudio 21, 80125 Napoli, Italy*

^c*Dipartimento di Fisica, Università di Napoli Federico II, RISSC – Lab Via Coroglio 156, 80124 Napoli, Italy*

Received 2 March 2007; received in revised form 7 July 2007; accepted 15 July 2007

Abstract

The development and implementation of an earthquake early warning system (EEWS), both in regional or on-site configurations can help to mitigate the losses due to the occurrence of moderate-to-large earthquakes in densely populated and/or industrialized areas. The capability of an EEWS to provide real-time estimates of source parameters (location and magnitude) can be used to take some countermeasures during the earthquake occurrence and before the arriving of the most destructive waves at the site of interest. However, some critical issues are peculiar of EEWS and need further investigation: (1) the uncertainties on earthquake magnitude and location estimates based on the measurements of some observed quantities in the very early portion of the recorded signals; (2) the selection of the most appropriate parameter to be used to predict the ground motion amplitude both in near- and far-source ranges; (3) the use of the estimates provided by the EEWS for structural engineering and risk mitigation applications.

In the present study, the issues above are discussed using the Campania–Lucania region (Southern Apennines) in Italy, as test-site area. In this region a prototype system for earthquake early warning, and more generally for seismic alert management, is under development. The system is based on a dense, wide dynamic accelerometric network deployed in the area where the moderate-to-large earthquake causative fault systems are located.

The uncertainty analysis is performed through a real-time probabilistic seismic hazard analysis by using two different approaches. The first is the Bayesian approach that implicitly integrate both the time evolving estimate of earthquake parameters, the probability density functions and the variability of ground motion propagation providing the most complete information. The second is a classical point estimate approach which does not account for the probability density function of the magnitude and only uses the average of the estimates performed at each seismic station.

Both the approaches are applied to two main towns located in the area of interest, Napoli and Avellino, for which a missed and false alarm analysis is presented by means of a scenario earthquake: an M 7.0 seismic event located at the centre of the seismic network.

Concerning the ground motion prediction, attention is focused on the response spectra as the most appropriate function to characterize the ground motion for earthquake engineering applications of EEWS.

© 2007 Elsevier Ltd. All rights reserved.

Keywords: Earthquake early-warning; Real-time seismology; Bayesian analysis; Missed and false alarm

1. Introduction

The purpose of an earthquake early warning system (EEWS) is to provide real-time notification of ground shaking before the arriving of the potentially destructive waves at the site of interest. This system requires a dense seismic network, a telemetered communication system, a central data processing unit and a notification system [1,2].

The scientific base on which the concept of early-warning relays is provided by real-time seismology, which faces the problem of estimating magnitude and location of an earthquake from the very beginning of the rupture process. Concerning real-time magnitude estimation, several methods have been developed in recent years. This is the case, for example, of the method proposed by Allen and Kanamori [3] based on the measurement of the predominant period ($\tau_{P, \max}$) in the few seconds after the *P*-wave arrival onset, or that proposed by Wu and Zhao [4] based on the peak displacement amplitude measured in the first

*Corresponding author. Tel.: +39 081 2420318; fax: +39 081 2420334.
E-mail address: convertito@ov.ingv.it (V. Convertito).

3 s after the arrival of the P -wave. More recently Zollo et al. [5] have proposed a technique for magnitude estimation based on the measurement of early peak amplitude of the P - and S -wave signals. On the other hand, real-time earthquake location techniques have been proposed by Horiuchi et al. [6], Rydelek and Pujol [7] and more recently by Satriano et al. [8]. These techniques are all based mainly on the equal differential-time (EDT) formulation and use information about the number of triggered and not yet triggered stations at a given time, in order to define Voroni cells. These cells are volumes in which the probability of finding the earthquake hypocenter is the higher. Aside from the different variations characterizing the previous techniques, all agree about the possibility of locating an earthquake in 4–5 s from its origin time.

Worldwide installation of EEWs is now driving seismologists and engineers to face with the problem of studying the reliability of the real-time estimates of the ground-shaking performed by the systems near and far from the seismic source area, and in particular in the regions not covered by the seismic network. In fact, most of the countermeasures, both automatic or not, aimed at reducing the potential impact of destructive earthquakes on the society, are based on these estimates. The prediction of the ground-shaking at a site of interest consists of the values of one or more ground motion parameters obtained by using specific tools. The most used prediction tools are the attenuation relationships [9,10], that are mathematical functions relating earthquake parameters (e.g. magnitude or seismic moment), source-to-site distance and site effect,

with peak ground motion parameters (e.g. peak ground acceleration (Pga), peak ground velocity (Pgv)) and spectral ordinates (e.g. spectral acceleration (S_a), spectral velocity (S_v)) or simulation techniques able to account for many more details of the rupture process (e.g. [11]). However, aside from the reliability and the rapidity of the estimates related to the use of the previous estimating tools, providing only the value of the strong-ground motion parameters, can have a little meaning if not accompanied by uncertainties.

In recent papers, Iervolino et al. [12] have developed a new technique which allows to account for the uncertainties carried by the real-time estimates of earthquake's characteristics and extended the analysis not only to the prediction of ground motion but also to the expected loss based on the main feature of the EEWs [13] in *hybrid* configuration. That is, a configuration where the seismic network is located around the potential fault system and strong-ground motion estimates are needed at a site far from the source region [2]. The technique is based on a Bayesian approach that allows to perform ground motion estimates in terms of probability density functions (pdfs) similar to the classical probabilistic seismic hazard analysis (PSHA) proposed by Cornell [14]. The basic idea is to benefit from the results of the real-time seismology, concerning both magnitude and location of the impending earthquakes, in a Bayesian framework. Iervolino et al. [12] used as test area the Campania–Lucania region in Southern Apennines (Italy) (Fig. 1) where a dense, wide dynamic accelerometric network, mainly devoted to early-warning applications is under development [15] and focused their

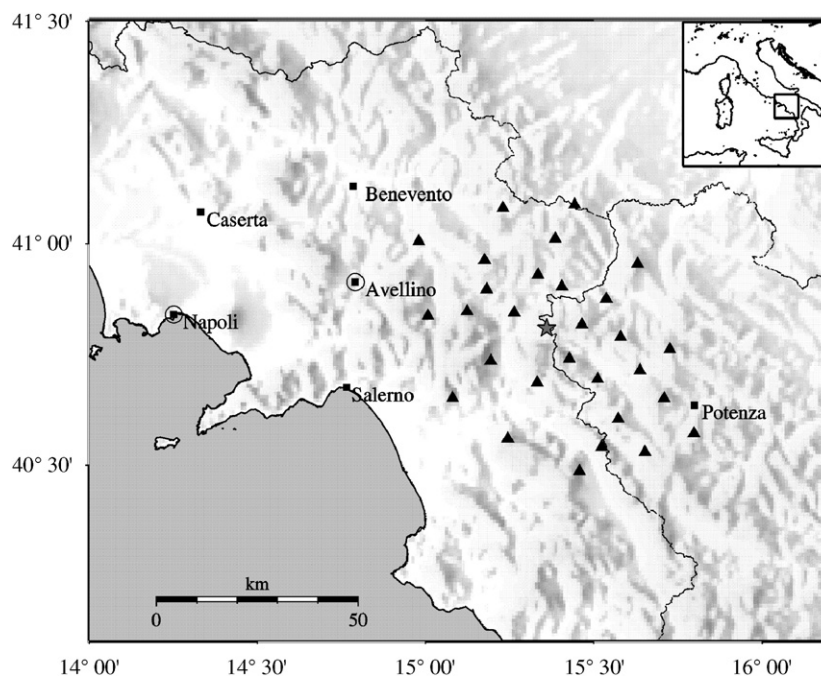


Fig. 1. Map of the area test selected for the analyses. Squares represent the main towns of the Campania–Lucania region (Southern Apennines) Italy. The black triangles represent the stations of the ISNet network while the grey star corresponds to the epicentre of the M 7.0 event selected as scenario earthquake.

attention to missed and false alarms study limited only to Pga. In the present paper, the Bayesian approach is extended to the spectral ordinates that represent the most appropriate functions to characterize the strong-ground motion for earthquake engineering applications of EEWS. In fact, it is the intensity measure used by the Performance-based Earthquake Engineering [12] to better characterize the structural seismic response in respect to the peak ground acceleration. In fact, Pga may be useful to predict the response of non-structural elements, but may be statistically insufficient for some demand measures for buildings as the peak interstory drift ratio. In order to compare the differences between the two approaches, also a classical point estimate approach is used, which differs from the Bayesian one because it uses as real-time magnitude value at a given instant of time the average of the estimates at each seismic station. The analysis is performed for two selected sites located at two main towns of the Campania–Lucania region, that are Napoli and Avellino (Fig. 1), for which the results of the real-time estimation of missed and false alarm probabilities are also presented.

2. Real-time prediction of response spectra

2.1. The Bayesian approach for magnitude estimation

Real-time risk analysis is based on the ability of the EEWS, particularly in regional configuration [2], to measure earthquake parameters in the seismic source area in the early stage of the rupture process and to estimate the values of the selected strong-ground motion parameters at a site located far from the source. In order to develop optimal alarm decision analysis, which accounts also for the trade-off between false and missed alarm probabilities, a study of the uncertainties on the estimates is of main concern. In first instance, assuming that the peak ground motion parameters are governed by log-normal pdfs (e.g. [16]) it could be possible to compute exceeding probabilities of some threshold values selected on the basis of the specific structure of interest. Although of great utility, this information does not account for the uncertainties linked to the ability of the EEWS to provide time-evolving estimates of magnitude and location of the impending earthquake which are governed by their own pdfs. In the present paper, the approach limited to estimate single values of the selected strong-ground motion parameter is overcome by using a Bayesian approach. This approach allows to retrieve the whole pdf of the selected parameter by using a modified formulation of the hazard integral used in the classical probabilistic hazard analyses [14] and, in particular, to provide these pdfs conditioned to the real-time information provided by the EEWS. This is the base for the modification of the classical hazard integral, in so far as, both the mean values and the uncertainties of those parameters mainly depend on the information provided by the EEWS during the occurrence of the earthquake. The

generalized formulation of the hazard integral can be written as

$$f(S_a(T)) = \int_M \int_R f[S_a(T)|m, r] \times f_{M|\tau_1, \tau_2, \dots, \tau_{n_{\text{trig}}}}(m|\bar{\tau}_{n_{\text{trig}}}) \times f_{R|v_1, v_2, \dots, v_{n_{\text{trig}}}}(r, \bar{v}_{n_{\text{trig}}}) dr dm. \quad (1)$$

Eq. (1) thus provides the pdf of the spectral ordinates $S_a(T)$ of the response spectra for a set of structural periods T . The pdf $f(S_a(T))$ allows to obtain the most complete information, i.e., the modal value, the median value, the uncertainty or, as in the classical hazard analyses, the probability of exceedance of some threshold value. The main advantage of this formulation consists in its generality; it does not strictly depend on the adopted methodology for magnitude and location estimates although only for some cases it will be possible to write down analytical form for the corresponding pdfs. In the classical hazard analysis, the pdf on the magnitude is a truncated exponential function obtained from the Gutenberg–Richter relationship retrieved from the seismic catalogue collected in the earthquake source area of interest.

In the hazard integral $\tau_1, \tau_2, \dots, \tau_{n_{\text{trig}}}$ represent a vector of measures of some physical parameter at the n_{trig} recording stations of the seismic network in the early stage of the recorded signal. The pdf $f_{M|\tau_1, \tau_2, \dots, \tau_{n_{\text{trig}}}}(m|\bar{\tau}_{n_{\text{trig}}})$ thus provides the probability that, on the basis of the real-time measurements $\bar{\tau}_{n_{\text{trig}}}$, the occurring earthquake has a magnitude in a given range. A non trivial problem that has to be faced in formulating this pdf in a real-time approach, concerns the selection of the most appropriate a-priori information when a sufficient number of measurements is not yet available. This can be the case, for example, when some station does not correctly work, or the earthquake is located on the edge or outside the region covered by the seismic network. As shown by Iervolino et al. [12], when the measurements $\bar{\tau}_{n_{\text{trig}}}$ are the predominant period $\tau_{P, \text{max}}$ of the first 4s of the P -waves proposed by Allen and Kanamori [3], and the a-priori information is the Gutenberg–Richter ($e^{-\beta m}$) relationship, the pdf on the magnitude has an analytical formulation that, using the Bayesian approach, for a given magnitude range ($M_{\text{min}}, M_{\text{max}}$) is given by

$$f_M(m|\tau_1, \tau_2, \dots, \tau_{n_{\text{trig}}}) = \frac{e^{\{2\mu_{\log(\tau)} \left[\sum_{i=1}^{n_{\text{trig}}} \log(\tau_i) \right] - n_{\text{trig}} \mu_{\log(\tau)}^2 / 2\sigma_{\log(\tau)}^2\}} e^{-\beta m}}{\int_{M_{\text{min}}}^{M_{\text{max}}} e^{\{2\mu_{\log(\tau)} \left[\sum_{i=1}^{n_{\text{trig}}} \log(\tau_i) \right] - n_{\text{trig}} \mu_{\log(\tau)}^2 / 2\sigma_{\log(\tau)}^2\}} e^{-\beta m} dm}. \quad (2)$$

The numerator in Eq. (2) represents the probability of measuring a set of $\bar{\tau}_{n_{\text{trig}}}$ given that an earthquake of magnitude m is occurring, i.e., $(m|\bar{\tau}_{n_{\text{trig}}})$ multiplied by the a-priori pdf. Note that, formulating Eq. (2) requires the assumption of s -independence and homoskedasticity of the

logs of the measurements and that the distributions of the components of the vector $\bar{\tau}_{n_{\text{trig}}}$, conditioned to the magnitude of the earthquake, i.e., $f_{\tau|M}(\tau|m)$, are log-normal characterized by the parameters reported in the following equations:

$$\begin{cases} \mu_{\log(\tau)} = (M - 5.9)/7, \\ \sigma_{\log(\tau)} = 0.16. \end{cases} \quad (3)$$

The value $\mu_{\log(\tau)}$ is provided by Allen and Kanamori [3] while the value of the dispersion $\sigma_{\log(\tau)}$ has been retrieved by using the data provided by Allen and Kanamori [3] in the same paper.

Fig. 2 shows the time evolving estimation of the $f_M(m|\bar{\tau}_{n_{\text{trig}}})$ for an M 6.0 earthquake (grey lines) along with the a-priori distribution on the magnitude obtained from the Gutenberg–Richter relationship (black line). The results reported in Fig. 2 have been obtained by selecting an earthquake located at the centre of the seismic network. This allowed to test possible effects concerning the seismic network configuration.

The parameters used to compute the Gutenberg–Richter relationship and the pdf on the magnitude for the region of interest are $\beta = 1.69$, $M_{\text{min}} = 4.0$ and $M_{\text{max}} = 7.0$.

Note how both the median value and the width of the pdf change with the increasing number of triggered stations (n_{trig}), that represents the increasing amount of information coming from the EEWs.

For a set of triggered stations $v_1, v_2, \dots, v_{n_{\text{trig}}}$, the function $f_{R|v_1, v_2, \dots, v_{n_{\text{trig}}}}(r|\bar{v}_{n_{\text{trig}}})$ represents the pdf on the source-to-site distance. This pdf accounts for two different information, that are, the time evolving location and the identification of a volume inside which the hypocenter is located with a given probability. As a consequence, there is an implicit dependence on the selected location technique. In the present paper, the technique proposed by Satriano et al. [8] has been used which is an extension of the methodology proposed by Horiuchi et al. [6]. It allows to estimate the hypocenter probabilistically as a pdf instead of a point, and uses the EDT approach throughout to incorporate the triggered arrivals and the not yet triggered stations.

Moreover, it applies a full, global search for each update of the location estimate and starts the location procedure after only one station has triggered. From a real-time risk analysis point of view, the most interesting feature of the methodology concerns the possibility to identify probabilistic volumes where hypocenters are located by using a stacking of the EDT surfaces between pairs of triggered and not yet triggered stations. These surfaces are defined as isochrone surfaces with respect to *P*-wave travel times. Except for simple cases in which the volume is reduced to a point, a line or a circle, the difficulty remains to write the $f_{R|v_1, v_2, \dots, v_{n_{\text{trig}}}}(r|\bar{v}_{n_{\text{trig}}})$ in an analytical form as for the magnitude.

Finally, the pdf $f[S_a(T)|m, r]$ is the conditional probability of exceedance for a given magnitude distance couple (m, r) deduced from the attenuation relationship and based on the assumption of a log-normal distribution of the $S_a(T)$ parameter (e.g. [16]). In the present application the attenuation relationship refers only to rock site condition. However, when site-specific transfer function are available for the site of interest, a correction of $f(S_a(T))$ can be performed.

A problem that has to be faced in defining the pdf $f[S_a(T)|m, r]$ is the fact that, although recent development (e.g. [17,18]), all the classical attenuation relationships have a constant standard error of the logs with respect to magnitude and distance. However, when the risk analysis is devoted to estimate response spectra, as in the present paper, a further feature can be investigated. This concerns the fact that the standard error depends on the selected structural period.

2.2. The classical point estimate approach

In order to understand if there is an uncertainty between that corresponding to the magnitude or to the attenuation relationship, that mainly governs the shape of $f(S_a(T))$ it is worthwhile to apply also a classical point estimate approach. This approach is based on the inversion of the first of the Eq. (3) and the averaging of the estimates at all

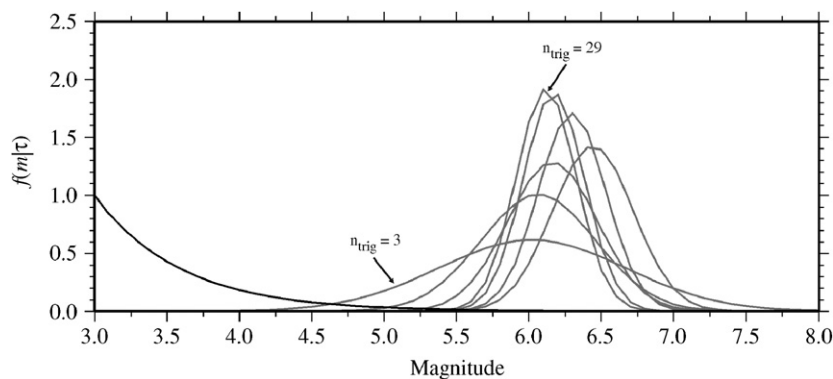


Fig. 2. Time evolution of the pdfs of the magnitude (grey lines) for an M 6.0 earthquake located at the center of the network. Black line represents the pdf on the magnitude retrieved from the Gutenberg–Richter relation for the region of interest and used as a-priori information.

the n_{trig} stations. This corresponds to obtain the average of the magnitude provided by each station, i.e.,

$$M = \frac{\sum_{i=1}^{n_{\text{trig}}} [7 \log(\tau_i) + 5.9]}{n_{\text{trig}}} \quad (4)$$

In Fig. 3 are reported the results for 1000 simulations obtained by applying both the approaches to an M 7.0 earthquake located at an epicentral distance of 90 km. Each curve represents the final response spectrum, i.e., when all the seismic stations have triggered.

Triggering times are evaluated by computing P -wave travel-times assuming an isotropic and homogeneous medium having a velocity $v_p = 5.5$ km/s. The selected real-time location procedure [8] incorporates uncertainty which is assumed to be negligible, with respect to that of the magnitude and attenuation relationship after 4 s from the first trigger. Since the magnitude estimation procedure also requires at least 4 s of recorded signal, the real-time response spectrum prediction, in the application presented in this paper, starts after 4 s from the first trigger.

Panels *a* and *c* show the median response spectra obtained from Bayesian and classical point estimate approaches, respectively, at the instant of time in which all the stations of the seismic network have triggered ($n_{\text{trig}} = 29$). The grey line in the same panels represents the response spectra computed by using only the Sabetta and Pugliese [19] (hereinafter SP96) attenuation relationship that corresponds to the expected spectrum and, fixed the magnitude and the location of the earthquake, represents the maximum status of knowledge. The histograms reported in panels *b* and *d* show the distributions of the $S_a(T)$ values for the structural periods reported in the labels. The vertical lines in each panel correspond to the value of $S_a(T)$ computed by using the SP96 attenuation relationship. The results reported in these figures allow to verify that the two approaches provide similar modal values of the response spectra, and somewhat different variability. Such variability depends on the selected structural period which is mainly correlated with the standard errors provided by the SP96 attenuation relationship. However, the most interesting feature is that, aside from the used approach, all the spectra distribute around the spectrum corresponding to the maximum status of knowledge, i.e., when magnitude and location of the earthquake are known. Moreover, the fact that the two approaches provide similar values of the dispersion suggests that the uncertainty that mainly affects the final estimates is that corresponding to the attenuation relationships rather than that related to the magnitude's estimation.

2.3. The missed and false alarm issue

Missed and false alarm probabilities are generally defined starting from the selection of a decision rule. This rule is used to launch the alarm or not, once the EEWS has provided the distribution of the ground motion parameter.

A possible decision rule is reported as follows:

$$\text{Alarm} = 1 - \int_0^{S_a^c(T)} f(S_a(T)) dS_a = P[S_a(T) > S_a^c(T)] > P_c \quad (5)$$

This formulation is based on the assumption that alarm is launched if the probability of S_a at the structural period T of interest exceeding a critical threshold value $S_a^c(T)$ outcrosses a reference value P_c . The P_c and $S_a^c(T)$ values are selected in relation to an appropriate loss function for the structure of interest and the acceptable probabilities of errors in the decisions [12]. The efficiency of the decision rule may be tested in terms of false and missed alarm probabilities, P_{FA} and P_{MA} , respectively [20]. In particular, the false alarm occurs when the alarm is issued while the strong-ground motion parameter at the site S_a^T is lower than the threshold value. On the other hand, the missed alarm corresponds to not launching the alarm if needed. In the application presented in this paper, false and missed alarms are defined separately for spectral ordinates at each fundamental period:

$$\begin{cases} \text{Missed Alarm :} & [\text{No Alarm} \cap S_a^T(T) > S_a^c(T)], \\ \text{False Alarm :} & [\text{Alarm} \cap S_a^T(T) \leq S_a^c(T)]. \end{cases} \quad (6)$$

The application of Eq. (1) to EEWS systems provides real-time estimates of the pdf that governs the selected strong-ground motion parameter. Because the shape of this pdf depends on the number of triggered stations n_{trig} at a given instant of time, it is thus possible to evaluate false and missed alarm probabilities in a time-dependent approach. As a consequence, the amount of information collected on the event and the available lead time that is the amount of time between the receipt of the first information about the impending earthquake and the arrival of the seismic phase of interest, represent a trade-off which should be accounted for in alarming decision.

In the present paper, missed and false probabilities analysis has been performed at two main towns of the Campania–Lucania region (Southern Apennines, Italy), in particular Napoli and Avellino (Fig. 1). This allowed to test how these probabilities depend on the threshold values, on the selected critical spectrum, on the source-to-site distance and the time from the first trigger.

3. Application to the Campania–Lucania region (Southern Apennines), Italy

The analysis concerning both the real-time response spectrum estimation and the missed and false alarm issue has been performed by using a simulation approach (e.g. Monte Carlo). During the simulations, the measurements of the parameters of interest are randomly extracted from their pdfs. This is the case for example for $\tau_{P,\text{max}}$ [3] and $S_a^T(T)$.

The selected test area is the Campania–Lucania region (Southern Apennines) in Italy, where a prototype EEWS is

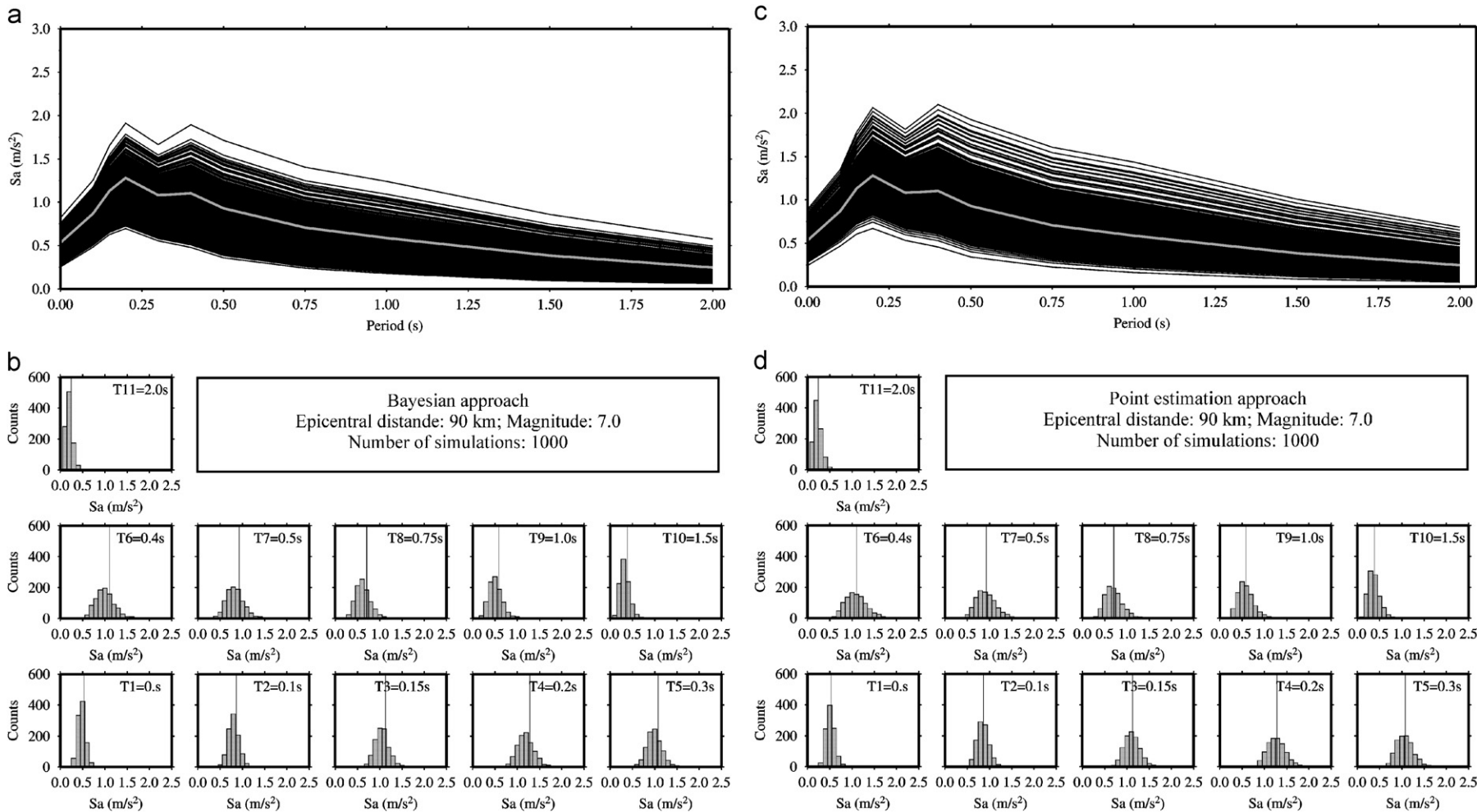


Fig. 3. Estimated median response spectra corresponding to the instant of time in which all the stations have triggered. Panel a shows the results of 1000 simulations when Bayesian approach is used. Grey line correspond to the response spectrum estimated by using the SP96 attenuation relationship. Panel c shows the same results when classical point estimate approach is used. Panels b and d show the distributions of the estimated and predicted (vertical line) $S_a(T)$ values for each structural period.

under development. The system is based on a dense, wide dynamic network named ISNet [15] which encloses the seismogenetic structures that originate the last destructive earthquake occurred in the region on 23 November 1980 (M 6.9). The ISNet configuration is reported in Fig. 1 (triangles) along with the main towns which represent potential sites of interest (black squares). For the selected region, the parameters used to compute the Gutenberg–Richter relationship and, as a consequence, the pdf on the magnitude which is the a-priori information in Eq. (2) are $b = 0.7356$ ($\beta = b \ln 10$), $M_{\min} = 3.0$ and $M_{\max} = 7.0$. The grey star in Fig. 1 represents the epicentre of the selected M 7.0 earthquake while the circles indicate the two

main towns Napoli and Avellino chosen as sites of interest for the analysis located at epicentral distances of about 90 and 46 km, respectively.

Evaluating Eq. (6) requires the definition of a critical response spectrum $S_a^c(T)$ for each period of interest T . In the present application, for the two sites the critical spectrum has been computed by using the spectral shape for A-type site class given in the Eurocode 8 [21] evaluated at 11 different structural periods, i.e., $T = 0, 0.1, 0.15, 0.2, 0.3, 0.4, 0.5, 0.75, 1.0, 1.5, 2.0$ s. The anchoring values have been selected as the Pga values having a return period of 475 years that are 2.0 and 1.5 m/s^2 for the site of Avellino and Napoli, respectively [22].

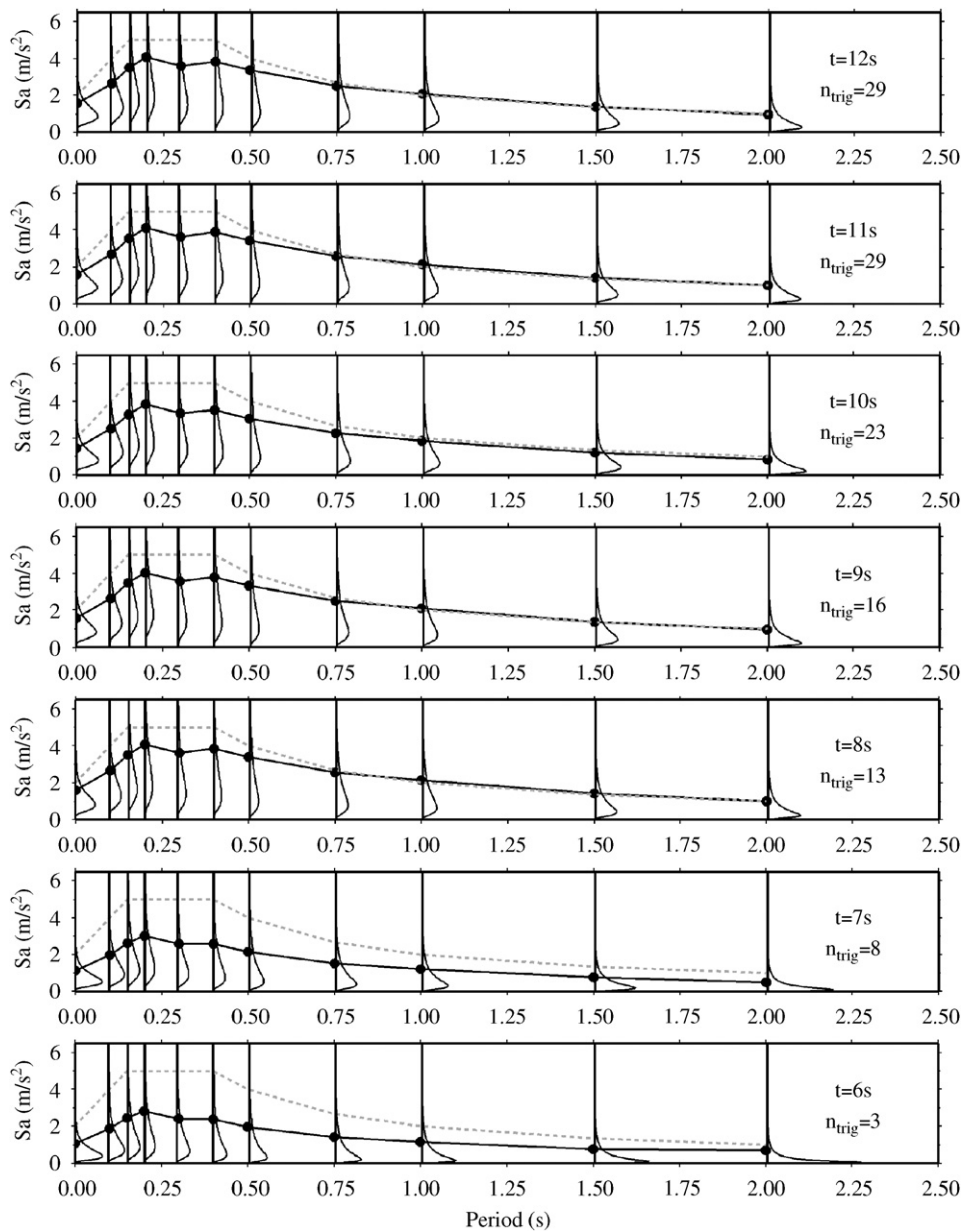


Fig. 4. Real-time response spectrum estimation for the site of Avellino (black lines) retrieved from the pdfs reported in the same figure obtained by using Bayesian approach. The labels report the corresponding instant of time and the number of triggered stations. Grey lines represent the critical spectrum computed following the Italian code for the site of Avellino.

In order to evaluate the $f(S_a(T))$ for each site, a number of 1000 simulations has been performed applying both the Bayesian and the classical point estimation approaches. Each simulation consists of: (1) selecting the earthquake characteristics (i.e., magnitude and location) and sampling the true values $S_a^T(T)$ at the site for each structural period from its distribution conditioned to the selected magnitude and distance pair; (2) simulation of the measurements and predictions made by the EEWs at each instant of time until all the stations have triggered; (3) check the decision rule and the false/missed alarm conditions.

Triggering times are computed according to the description given in the previous section. Fixed the earthquake magnitude, the τ_i measurements are sampled assuming that they are statistically independent and log-normally

distributed with mean value and dispersion reported in Eq. (3).

The $S_a^T(T)$ values for each period are obtained by sampling the pdf retrieved by using the median and the dispersion provided by SP96 attenuation relationship for the selected magnitude and epicentral distance. Moreover, the same attenuation relationship is used to compute the conditional exceeding probability $f[S_a(T)|m,r]$ reported in Eq. (1).

The selection of a high number of simulations for the same magnitude and location and the random extraction of the $S_a(T)$ values from the pdf obtained from the selected attenuation relationship, implicitly allowed to account for the effect of different fault mechanisms particularly for the site of Napoli for which the large epicentral distance

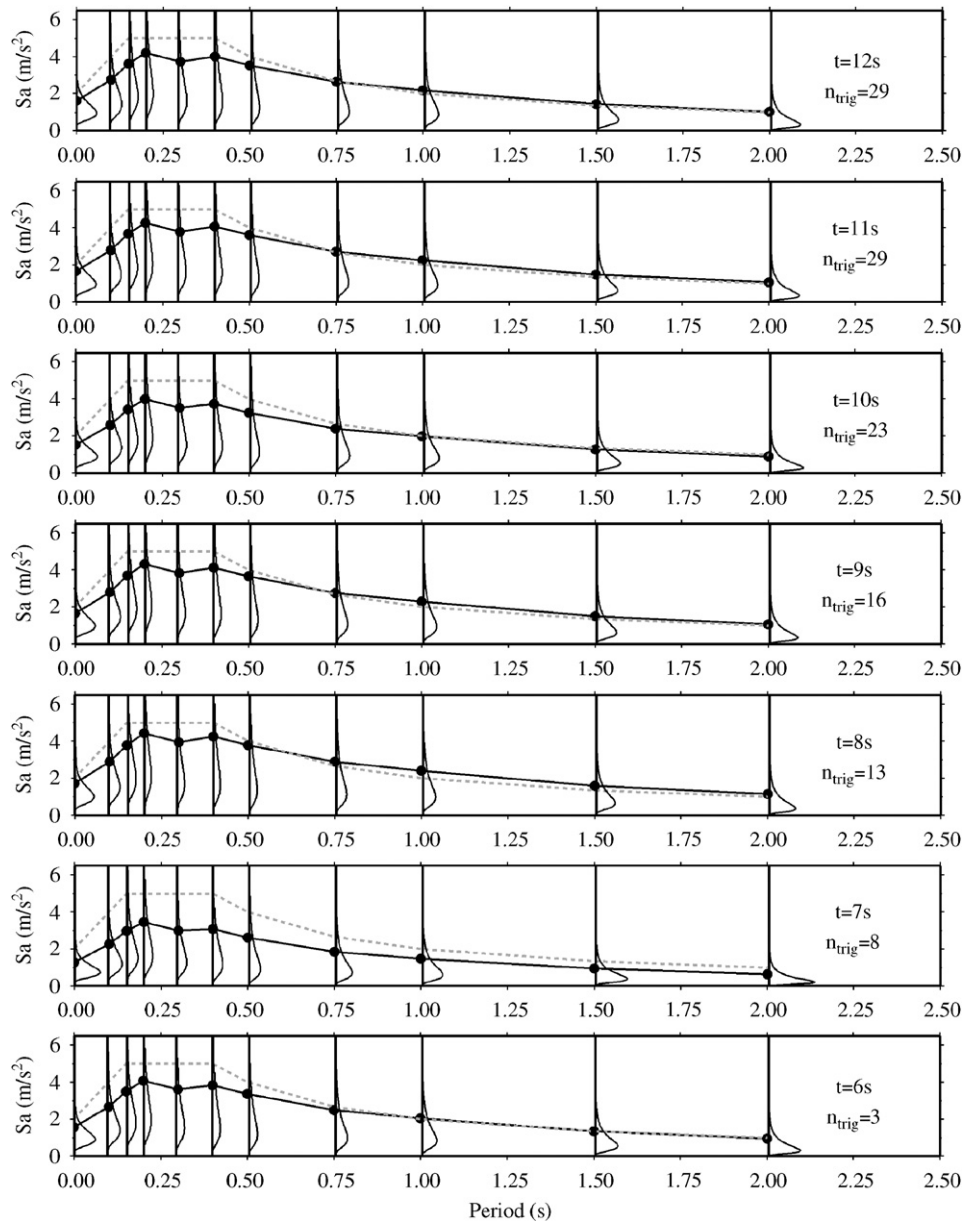


Fig. 5. Same as Fig. 4 but using the classical point estimate.

allowed to neglect the fault dimension. In fact, from a statistical point of view, the uncertainty provided by the attenuation relationships accounts for all the effects that can modify the values of the selected strong-ground motion parameter different from magnitude and source-to-site distance.

3.1. Results for Avellino

The first analysis concerned the real-time estimate of the response spectrum for the site of Avellino (Fig. 1). For the assumed homogeneous and isotropic velocity model ($v_p = 5.5 \text{ km/s}$; $v_s = v_p/\sqrt{3}$) P - and S -wave travel times are, respectively, $t_p = 8.5 \text{ s}$ and $t_s = 14.5 \text{ s}$. Assuming 4 s as time required to locate the earthquake by the selected location technique, the resulting lead time is about 8 s.

Figs. 4 and 5 report the results for one of the 1000 simulations obtained by using the Bayesian and point estimate approaches, respectively. The grey dashed lines correspond to the critical response spectrum while continuous black lines represent the spectrum estimated in real-time. The spectrum at each structural period was obtained by choosing a 20% of critical probability P_c . This probability value was selected because it is the value that will be used later in the analysis to evaluate the probability of missed and false alarm.

On each panel, the elapsed time from the origin time of the earthquake, along with the corresponding number of stations that have recorded the parameter used to compute the magnitude, is reported. In order to compare the results obtained via the two approaches, the spectra have been

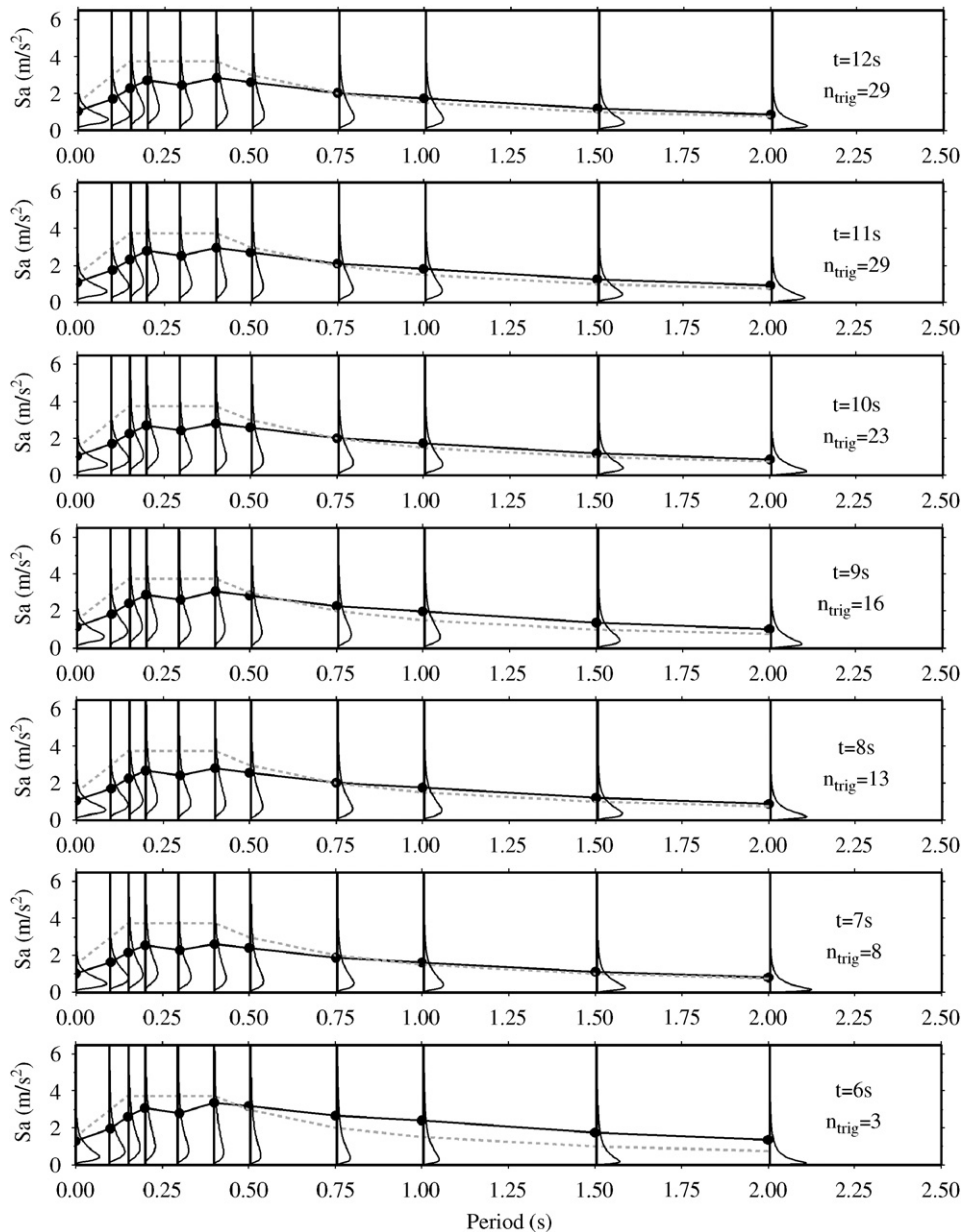


Fig. 6. Same as Fig. 4 but for the site of Napoli.

computed by fixing the same seed in the random number generator. For each period, also the corresponding $f(S_a(T))$ is shown allowing to analyse its variation with the time and the structural period. The variations both in terms of mean values and dispersions can be mainly attributed to the different dispersions provided by the SP96 attenuation relationship for each period, and also to the pdf on the magnitude.

Comparing the results reported in Figs. 4 and 5, note the different dispersion of the $f(S_a(T))$ between the two approaches and during the increasing time from the earthquake origin time assumed as zero reference time. Moreover, the spectra obtained by applying the Bayesian approach are slightly, but systematically lower than those

obtained by using the classical point estimate approach. This is in agreement with the fact that Bayesian estimators are not statistically correct. Lowermost panels of Figs. 4 and 5 indicate that the differences in the shape of the $f(S_a(T))$ are particularly evident in the early seconds, i.e., when only raw magnitude estimates are available while those corresponding to the final instant of time $t = 12$ s from the earthquake origin time, when all the stations have triggered, are quite similar.

3.2. Results for Napoli

The same analysis performed at Avellino has been applied at the site in Napoli by using both Bayesian and

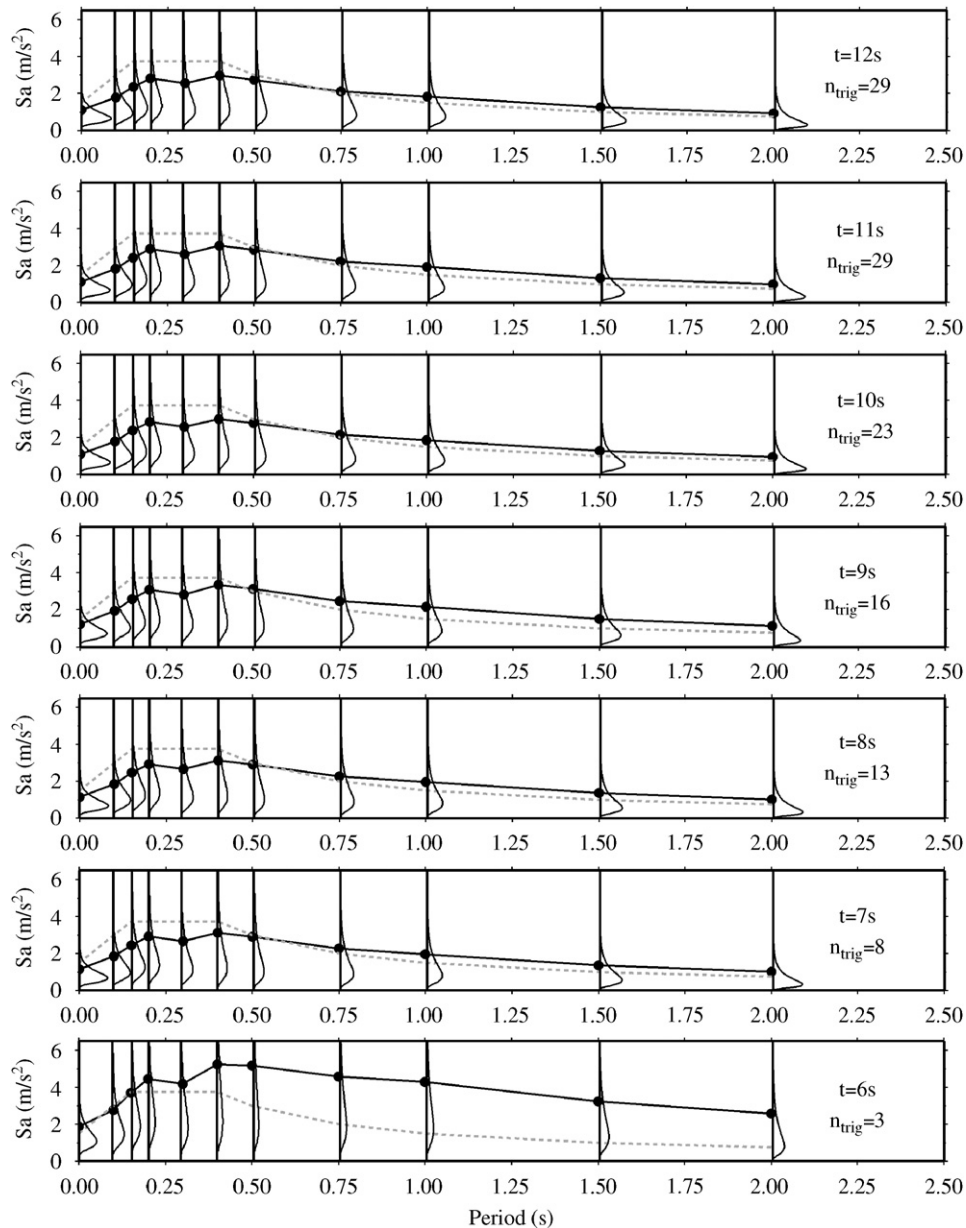


Fig. 7. Same as Fig. 6 but using the classical point estimation.

classical point estimate approaches. This allowed to underline possible effects on the results of both the source-to-site distance and the critical spectrum. Figs. 6 and 7 show the time evolution of the estimated response spectra along with the corresponding $f(S_a(T))$. Using the same assumptions on the velocity model for the site of Napoli, P - and S -wave travel times are, respectively, $t_P = 16.4$ s and $t_S = 28.3$ s and the lead time is about 20 s.

Also for the site in Napoli, the estimated spectra are different when the two approaches are applied, but become similar starting from $t = 9$ s from the earthquake origin time. Comparing these results with those reported in the Figs. 4 and 5 corresponding to the site of Avellino, it is possible to note that almost all the $f(S_a(T))$ have a lower dispersion that can be attributed to the attenuation relationships effect.

3.3. The missed and false alarm issue

The simulating approach used to compute real-time response spectra is also used to compute the missed and false alarms having selected Eq. (5) as decision rule and, moreover, to compute the probabilities of missed (P_{MA}) and false alarm (P_{FA}) by using the frequency of occurrence of the corresponding alarms. These probabilities are reported in the following equation:

$$\begin{cases} P_{MA} \cong N[P(S_a(T) > S_a^c(T)) \leq P_c(T) \cap S_a^T(T) > S_a^c(T)] / N_{Simul}, \\ P_{FA} \cong N[P(S_a(T) > S_a^c(T)) > P_c(T) \cap S_a^T(T) \leq S_a^c(T)] / N_{Simul}. \end{cases} \quad (7)$$

where N_{Simul} is the number of simulations chosen as 1000 in the present application. For each structural period T , the

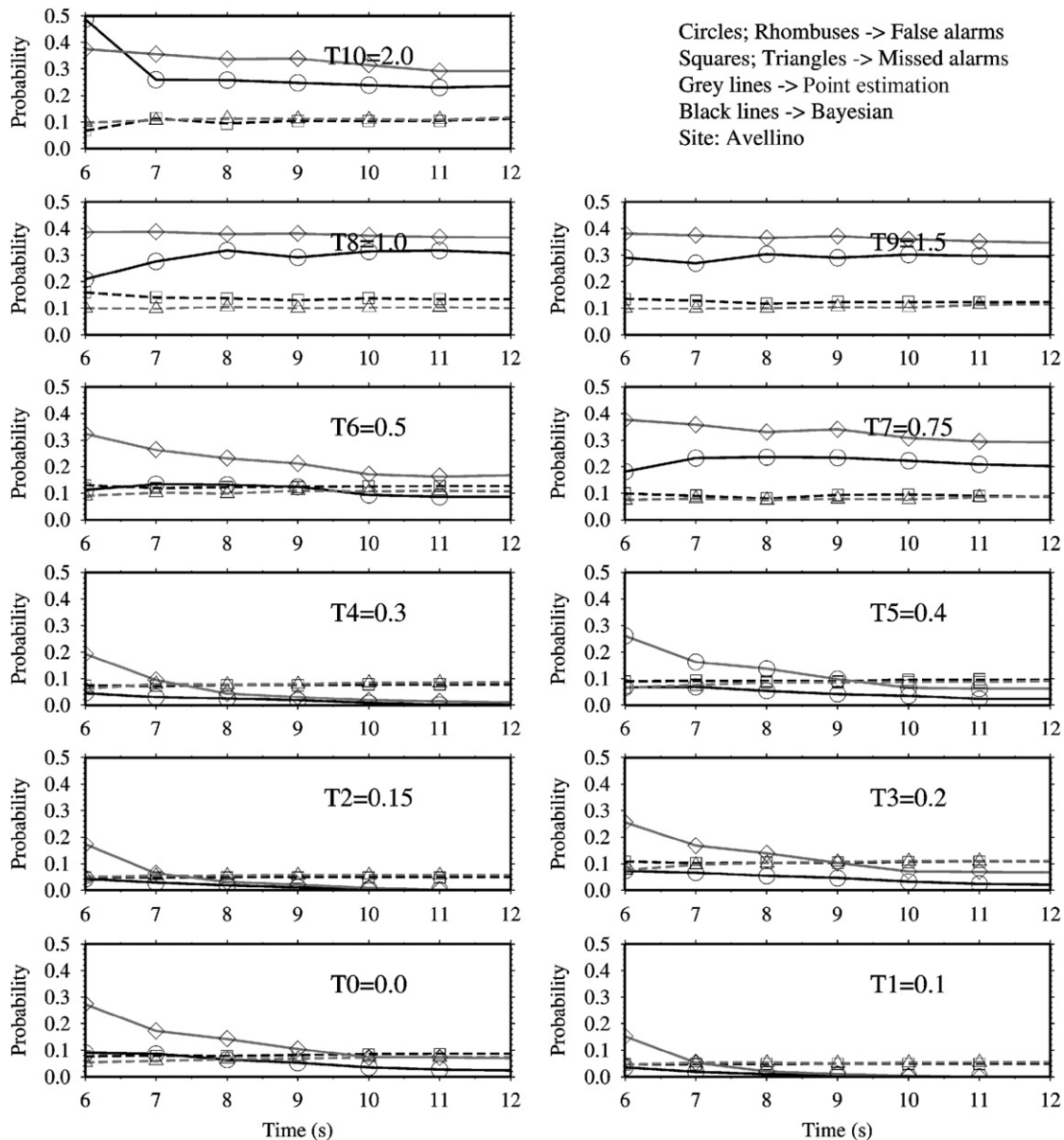


Fig. 8. Real-time estimation of missed and false alarm probabilities for each of the selected structural period for the site of Avellino. Black lines are the results obtained when the Bayesian approach is used while grey lines refer to the results obtained by using the classical point estimation.

critical probability P_c is fixed at 20% and the critical spectrum is computed according to the description given in the previous section. It is worthwhile to underline that false and missed alarm probabilities are computed at each structural period separately.

In the study presented by Iervolino et al. [12], the authors demonstrate that for an M 7.0 earthquake and a site located at an epicentral distance of 110 km, the probability of missed alarm for the Pga drops to 0 after 7s from the first trigger. On the other hand the probability of false alarm reaches the value corresponding to the case when magnitude and location are predicted by EEWs without uncertainties which, as consequence, may be considered the reference value for the system's performance.

In the present paper, the analysis has been extended to the whole response spectrum. Moreover, the selection of

two sites located at different epicentral distances to which correspond two critical spectra allowed to verify how P_{MA} and P_{FA} change as functions of these two variables. Figs. 8 and 9 show the results of the probabilities of missed and false alarms for the site of Avellino when both Bayesian and classical point estimation approaches are used and for all the selected spectral periods. Note that the differences in the shape (mean values and dispersions) of the $f(S_a(T))$ when the two approaches are used, have their effect on P_{MA} and P_{FA} for each selected period. In particular, aside from the particular selected site, P_{FA} has always lower values when the Bayesian approach is selected with respect to the point estimation approach. This is not true for P_{MA} that, for structural periods lower than 0.4 s are the same for the two approaches. Moreover, for the site of Napoli, for all the periods, both P_{MA} and P_{FA} converge to the same

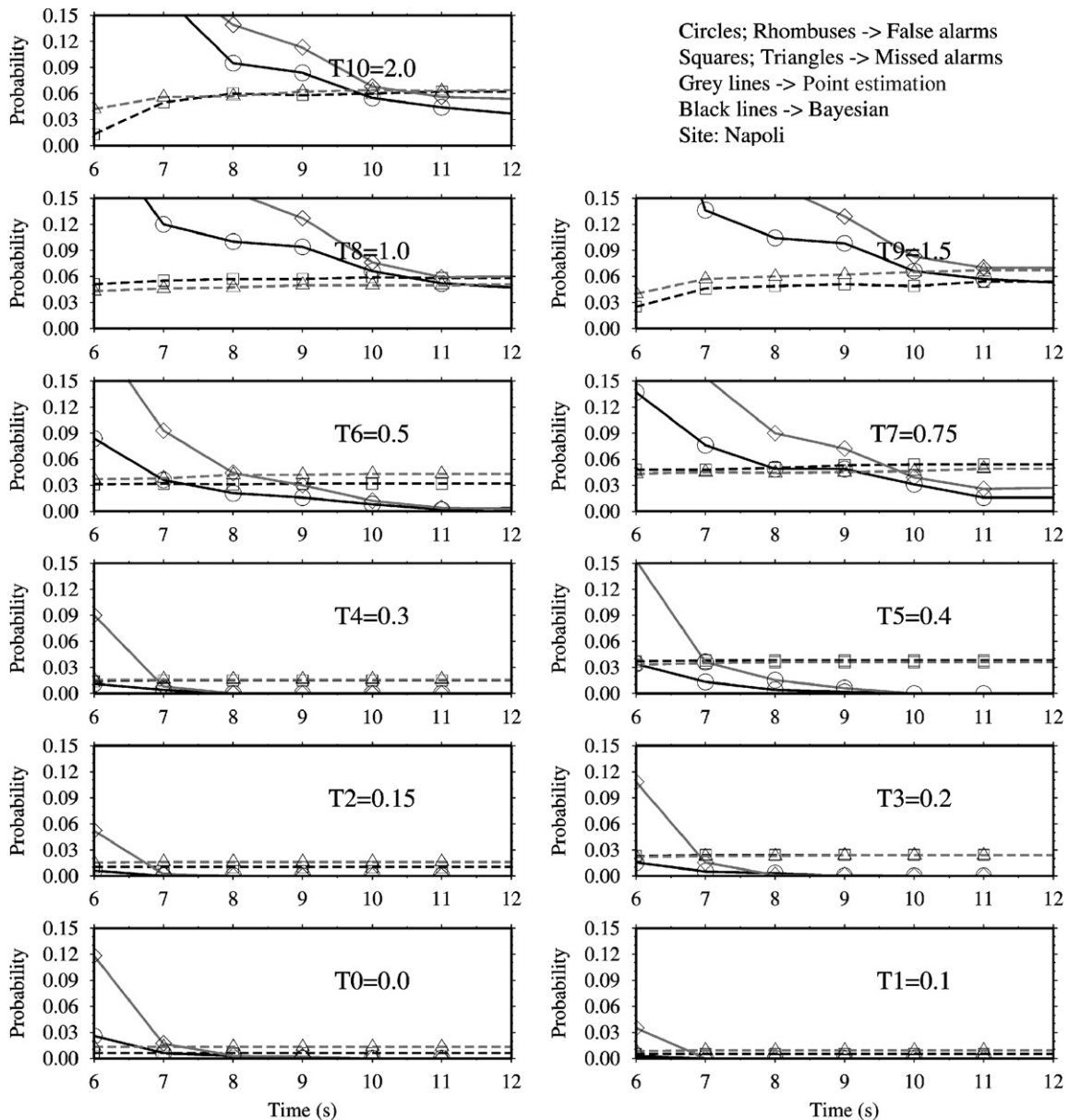


Fig. 9. Same as Fig. 8 but for the site of Napoli.

small values. On the other hand, for the site of Avellino, when the Bayesian approach is used (Fig. 8), the two probabilities are different also when all the seismic stations have triggered, and for larger periods ($T \geq 0.75$ s) the P_{MA} is always lesser than P_{FA} .

4. Conclusions

In the present paper the technique proposed by Iervolino et al. [12] aimed at real-time estimation of peak-ground motion has been extended to the whole response spectrum. The extension to the response spectra provides a most appropriate function to characterize the strong-ground motion for earthquake engineering applications of the EEWS. In fact, due to the dependence on the structural periods, it allows to better characterize the structural seismic response with respect to the P_{ga} .

In order to compare the results two approaches have been applied in the analysis. The first is the Bayesian approach proposed by Iervolino et al. [12] aimed at performing strong-ground motion estimates in terms of pdf similar to the classical PSHA proposed by Cornell [14] while the EEWS is gathering measurements about the impending earthquake. The second is a classical point estimate approach which does not account for the whole pdf on the magnitude.

The comparison between the two approaches has been carried out because Bayesian approach, for its own nature, may underestimate the strong-ground motion values, while the point estimation leads to larger uncertainty. However, by comparing the results obtained with two approaches shown in Fig. 3, note that, the Bayesian approach provides significantly smaller variability which is a desirable feature.

Furthermore, the comparison allowed to better understand which uncertainties mostly affect the estimated response spectra. The results have shown that for a 50% of critical probability P_c , aside from the used approach, the final response spectra, that is when all the stations have triggered, computed with 1000 simulations, distribute almost symmetrically around the expected spectrum, i.e., the spectrum computed by using the SP96 attenuation relationship for the true values of magnitude and location. This and other results allows to conclude that, the main source of variability is the attenuation relationship and its uncertainty.

However, the latter result may be conditioned by the assumptions made in the proposed approaches and on the parameter used by the EEWS for magnitude estimates. As an example, it may be useful to investigate the effect of the use of ground motion prediction relationships that account for dependency of the variance on magnitude.

In order to test the two approaches and compare the results, an application to the Campania–Lucania region (Southern Apennines), Italy is presented using as EEWS the one that is going to be installed in the area of interest named ISNet [15]. In particular, two main towns, that is Avellino and Napoli, have been selected as testing sites.

For each site, both Bayesian and point estimation approaches have been applied in order to evaluate the response spectra via real-time earthquake measurements. The selection of two sites located at different epicentral distances, which correspond to two different critical spectra, allowed to test the effect of the distance on the estimated spectra.

Furthermore, the analysis concerned the computation of the missed and false probabilities using as scenario an M 7.0 earthquake located at the centre of the seismic network. This analysis allowed to test how missed and false probabilities depend on the selected critical spectrum and on the epicentral distance. Moreover, due to the possibility of taking into account for the response spectrum, it has been tested how for the same earthquake scenario, i.e., same magnitude and epicentral distance, missed and false alarm probabilities depend on the structural period. The results showed that there is a dependence of the computed values of P_{FA} and P_{MA} both on the selected structural period and on the source-to-site distance. This is a consequence of the time variation of the dispersion of the $f(S_a(T))$ pdfs.

Acknowledgments

The figures were prepared with Generic Mapping Tools [23]. This work was financially supported by AMRA scarl (www.amra.unina.it) in the frame of the SAFER project (sixth framework programme sustainable development, global change and ecosystem priority 6.3.IV.2.1: reduction of seismic risks contract for specific targeted research or innovation project contract no. 036935) and in collaboration with the Italian Dipartimento della Protezione Civile in the frame of the ReLUIS project (2004–2006 Linea 9).

References

- [1] Heaton TH. A model for a seismic computerized alert network. *Science* 1985;228:987–90.
- [2] Kanamori H. Real-time seismology and earthquake damage mitigation. *Annu Rev Earth Planet Sci* 2004;33:5.1–5.20.
- [3] Allen RM, Kanamori H. The potential for earthquake early warning in Southern California. *Science* 2003;300:786–9.
- [4] Wu YM, Zhao L. Magnitude estimation using the first three seconds p-wave amplitude in earthquake early warning. *Geophys Res Lett* 2006;33:L16312.
- [5] Zollo A, Lancieri M, Nielsen S. Earthquake magnitude estimation from peak amplitudes of very early seismic signals on strong motion records. *Geophys Res Lett* 2006;33:L23312.
- [6] Horiuchi S, Negishi H, Abe K, Kanimura A, Fujinawa Y. An automatic processing system for broadcasting earthquake alarms. *Bull Seism Soc Am* 2005;95:708–18.
- [7] Rydelek P, Pujol J. Real-time seismic warning with a 2-station subarray. *Bull Seism Soc Am* 2004;94:1546–50.
- [8] Satriano C, Lomax A, Zollo A. Real-time evolutionary location for seismic early warning. *Bull Seism Soc Am* 2006 Submitted for publication.
- [9] Wald DJ, Quitoriano V, Heaton TH, Kanamori H, Scrivner CW, Worden CB. TriNet ShakeMaps: rapid generation of instrumental ground motion and intensity maps for earthquakes in southern California. *Earthquake Spectra* 1999;15:537–55.

- [10] Allen RM. The ElarmS earthquake warning methodology and application across California. In: Pecce M, Manfredi G, Zollo A, editors. In the many facets of seismic risk. Proceedings of the workshop on multidisciplinary approach to seismic risk problem, Sant'Angelo dei Lombardi, September 22, 2003. Università degli Studi di Napoli "Federico II"—CRdC-AMRA, 2004.
- [11] Dreger D, Kaverina A. Seismic remote sensing for the earthquake source process and near-source strong shaking: a case study of the October 16, 1999 Hector mine earthquake. *Geophys Res Lett* 2000;27:1941–4.
- [12] Iervolino I, Convertito V, Giorgio M, Manfredi G, Zollo A. Real-time risk analysis in hybrid early warning systems. *J Earthquake Eng* 2006;10(6):867–85.
- [13] Iervolino I, Giorgio M, Manfredi G. Expected loss-based alarm threshold set for earthquake early warning system. *Earthquake Eng Struct Dyn* 2007;36(9):1151–68.
- [14] Cornell CA. Engineering seismic risk analysis. *Bull Seism Soc Am* 1968;58:1583–606.
- [15] Weber E, Iannaccone G, Zollo A, Bobbio A, Cantore L, Corciulo M, et al. Development and testing of an advanced monitoring infrastructure (ISNet) for seismic early-warning applications in the Campania region of southern Italy. In: Gasparini et al., editors. *Earthquake early warning systems*. Berlin: Springer; 2007.
- [16] Reiter L. *Earthquake hazard analysis—issues and insights*. New York: Columbia University Press; 1990. 254pp.
- [17] Akkar S, Bommer JJ. Prediction of elastic displacement response spectra in Europe and the Middle East. *Earthquake Eng Struct Dyn* 2007;36(10):1275–301.
- [18] Ambraseys NN, Douglas J, Sarma SK, Smit P. Equations for the estimation of strong ground motions from shallow crustal earthquakes using data from Europe and the Middle East: horizontal peak ground acceleration and spectral acceleration. *Bull Earthquake Eng* 2005;3(1):1–53.
- [19] Sabetta F, Pugliese A. Estimation of response spectra and simulation of nonstationarity earthquake ground motion. *Bull Seism Soc Am* 1996;86:337–52.
- [20] Patè-Cornell ME. Warning systems in risk management. *Risk Manage* 1986;6:223–34.
- [21] CEN, European Committee for Standardisation TC250/SC8/ [2003] Eurocode 8: design provisions for earthquake resistance of structures, Part 1.1: general rules, seismic actions and rules for buildings, PrEN1998-1.
- [22] Calvi GM, Stucchi M. *Mappe interattive della pericolosità sismica*. Distributed through the Internet 2006: URL: <<http://essel.mi.ingv.it>>.
- [23] Wessel P, Smith WHF. Free software helps map and display data. *EOS Trans Am Geophys Union* 1991;72(441):445–6.